IRTA
RECERCA | TECNOLOGIA AGROALIMENTÀRIES

This document is a postprint version of an article published in Anthropod Structure & Development© Elsevier after peer review. To access the final edited and published work see https://doi.org/10.1016/j.asd.2022.101168

Document downloaded from:

IRTA Pubpro
Open digital archive

Morphological description of the midgut tract and midgut-hindgut junction in the larvae of the spider crab *Maja brachydactyla* Balss, 1922 (Malacostraca: Decapoda)

In memoriam of Mercè Durfort.

Diego Castejón[1,2*], Guiomar Rotllant[3], Enric Ribes[4], and Guillermo Guerao[5]

[1]Centro de Maricultura da Calheta. 9370-135 Calheta, Madeira (Portugal)

[2]IRTA, Centre d' Aqüicultura, Ctra. del Poble Nou. 43540 Sant Carles de la Ràpita, Tarragona (Spain)

[3]CSIC, Institut de Ciències del Mar. 08003 Barcelona (Spain).

[4]Unitat de Biologia Cel·lular, Departament de Biologia Cel·lular, Fisiologia i Immunologia, Facultat de Biologia, Universitat de Barcelona. 08028 Barcelona (Spain).

[5]Independent Researcher. Barcelona (Spain).

***Corresponding author:** Diego Castejón. E-mail: diego.castejon.dcb@gmail.com; phone: +34 681 154 398; postal address: Centro de Maricultura da Calheta. 9370-135 Calheta, Madeira (Portugal)

Abstract

The midgut tract of the decapods is a digestive organ involved in the synthesis of peritrophic membrane, food transport, absorption of nutrients, and osmoregulation. The midgut tract has been described in detail in adult decapods, but little information is available regarding the morphology and ultrastructure of the midgut tract in larval stages. The present study describes the midgut tract and the midgut-hindgut junction of the larvae of the common spider crab *Maja brachydactyla* Balss, 1922 using techniques that included dissection, light microscopy, and electron microscopy. The study is mainly focused on the stages of zoea I and megalopa. The results obtained in this study showed that the larval midgut tract is a short and simple tube positioned anteriorly, between the stomach and the hindgut tract. During larval development, the maximum length of the midgut tract increased significantly, but no differences were found on either the maximum diameter or the morphological traits of the organ. The midgut tract is active at least ca. 12 h after hatching, as suggested by the presence of the peritrophic membrane in the lumen, the presence of abundant electro-dense vesicles in the cell apex, and the release of the vesicle content on the organ lumen. The midgut-hindgut junction is an abrupt transition between the midgut tract and the hindgut tract in which epithelial cells with mixed features of midgut and hindgut do not occur.

Keywords: Pancrustacea; larval development; merocrine activity; peritrophic membrane; midgut-hindgut junction

1. Introduction

The functional morphology of the digestive system of the decapods (Malacostraca: Euricarida: Decapoda) tends to be relatively uniform among the different taxa (Felgenhauer, 1992; Icely and Nott, 1992). The digestive system is divided in three basic sections: the foregut, positioned anteriorly and formed by the oesophagus and stomach; the midgut, positioned in the middle and formed by the midgut gland, midgut tract, and midgut caeca; and the hindgut, positioned posteriorly and formed by the hindgut tract and the anus (Milne-Edwards, 1834; Felgenhauer, 1992; Icely and Nott, 1992; Davie et al., 2015; Castejón et al., 2018a; Spitzner et al., 2018). The embryonic origin determines the features of each section of the digestive system, i.e. the foregut and hindgut derivate from the embryonic ectoderm and are characterized by epithelia covered by a cuticle lining; while the midgut derivate from the embryonic endoderm and it is characterized by secretory epithelia with brush border (Felgenhauer, 1992; Icely and Nott, 1992; Davie et al., 2015). The midgut tract of the decapods is usually described as a simple tube with columnar epithelium and located between the stomach and the hindgut tract (Felgenhauer, 1992; Icely and Nott, 1992; Davie et al., 2015; Spitzner et al., 2018), which role has been associated with the synthesis of the peritrophic membrane (Georgi, 1969; Holliday et al., 1980; Martin et al., 2006), transport of the ingested food (Gibson and Barker, 1979; Ceccaldi, 1989; Felgenhauer, 1992; Icely and Nott, 1992), absorption of nutrients (Talbot et al., 1972), and osmoregulation (Komuro and Yamamoto, 1968; Talbot et al., 1972).

Knowledge on the morphology of the midgut tract is important to differentiate non-feeding from feeding larval stages (Lovett and Felder, 1989; Nakamura and Seki, 1990), to realize histopathological studies (Kaushik and Kumar, 1998; Martin et al., 2004), and to develop commercial diets for species of aquaculture interest (Fontagné et al., 1998;

Bonaldo et al., 2006; Øverland et al., 2009). In decapods, the epithelium of the midgut tract has two cell types: digestive cells with columnar shape involved in secretory and absorptive activities; and small regenerative cells with oval shape probably involved in cell division and differentiation (Sonakowska et al., 2015; Sonakowska et al., 2016). The morphology and ultrastructure of the midgut tract has been studied and reviewed in adult decapods (Felgenhauer, 1992; Icely and Nott, 1992; Factor, 1995; Davie et al., 2015). However, in the larval stages the majority of the studies focused on the whole digestive system so the midgut tract received little attention (Schlegel, 1911; Talbot et al., 1972; Lovett and Felder, 1989; Mikami et al., 1994; Abrunhosa and Kittaka, 1997; Jantrarotai and Sawanyatiputi, 2005; Tziouveli et al., 2011). Recently, the midgut tract was described in the larvae of the freshwater shrimp *Neocaridina davidi* (Sonakowska-Czajka et al., 2021).

In this study, the larval stages of the common spider crab *Maja brachydactyla* Balss, 1922 were used as a model to describe the midgut tract in true crabs' larvae. The common spider crab inhabits the eastern Atlantic coast from the British Isles to the Sahara and SW Mediterranean Sea (Sotelo et al., 2008b; Abelló et al., 2014), being a species of commercial interest (Freire et al., 2002; Sotelo et al., 2008a). The larval development embraces two planktonic zoeal stages (zoea I and zoea II), and a single planktonic-benthic megalopa stage that metamorphoses into a benthic juvenile (Clark, 1986; Guerao et al., 2008). This species has been a useful model to describe several digestive organs during the larval stages, e.g. oesophagus (Castejón et al., 2018b), stomach (Castejón et al., 2015b, 2019b), midgut gland (Castejón et al., 2019a), midgut caeca (Castejón et al., 2022), and hindgut tract (Castejón et al., 2021).

84 The aim of the present study is to describe in detail the midgut tract during the larval
85 development of the common spider crab *Maja brachydactyla* Balss, 1922 and discuss its
86 potential role and importance in the digestion processes.

87 **2. Material and methods**

88 *2.1 Culture system and larval obtaining*

89 The adult specimens of *M. brachydactyla* were captured on the North Atlantic and
90 provided by the local supplier Cademar S. Coop. R. L. (Alcanar, Tarragona) in April
91 2014, transported to the Institut de Recerca i Tecnologia Agroalimentàries (IRTA)
92 facilities in Ebro Delta (Sant Carles de la Ràpita, Tarragona, Spain), and placed in 2,000
93 L cylindrical tanks maintaining a sex ratio of one male per 5–6 females, water renewal
94 rate of 3.5 m^3 h^{-1}, 12:12 h light dark photoperiod, and temperature of 18 ± 1 °C, and
95 salinity of 35 ± 1 g L^{-1}. Animals were fedwith frozen and fresh mussels (genus *Mytilus*).

96 The spawning occurred spontaneously and the free swimming larvae were gathered in
97 special collectors directly from the adult tanks. The larvae (zoeae I, 12 h post-hatching)
98 were placed in 600 mL glass beakers at an initial density of 30 larvae per beaker. The
99 beakers were placed inside 360 L tanks (96 x 96 x 40 cm) used as culture chambers
100 maintaining constant temperature (21 ± 1 °C) and salinity (35 ± 1 g L^{-1}), 12:12 h light
101 dark photoperiod, and fed with live *Artemia* sp. Kellogg, 1906 nauplii (INVE
102 Aquaculture Nutrition, Salt Lake UT, USA). Daily, the larvae were pipetted to beakers
103 with clean water and fresh food. The larval culture lasted 12 days, being finished when
104 the larvae settled and metamorphosed to juvenile.

105 *2.2 Larval sampling and analyses of the midgut tract growth*

106 The specimens from two beakers were sampled on a daily basis, distributed for either
107 dissection (10–20 specimens) or light microscopy (4–6 specimens), and fixed

accordingly (see "*Light microscopy study*" section). Larvae were also fixed for electron microscopy (12 zoea I, 0 days post-hatching; 12 megalopae, 10 days post-hatching; see "*Transmission electron microscopy (TEM) study*" section for details). The specimens selected for dissection were fixed in formaldehyde 4% and dissected using a Nikon SMZ800 stereomicroscope (Nikon Instruments Inc., Melville, NY, U.S.A.) and teasing needles. The maximum length, width and height of the midgut tract from 5.6 ± 0.9 specimens day^{-1} were measured using image analysis software (AnalySIS, SIS, Münster, Germany), in a total of 73 specimens. The average between the width and height was calculated as the maximum diameter of the midgut tract in each specimen.

The R software version 4.1.0 (R Development Core Team, 2021) was used to perform all the statistical analyses. A general linear model was used to show the daily variation of the midgut tract length during the larval development. A One-Way ANOVA (type II) was used to compare the variation in maximum length and diameter among different stages: zoea I (0 days post-hatching, as newly hatched), zoea II (3 days post-hatching, as newly moulted), megalopa (6 days post-hatching, as newly moulted), and megalopa (11 days post-hatching, a day before the moult to juvenile because enough juveniles were not obtained in day 12). The data met the ANOVA assumptions, being the homogeneity of variances tested using the Levene's test of the package "car 3.0-7" (Fox and Weisberg, 2019), and the normality of the residuals using the Shapiro-Wilk test. The post hoc Tukey's HSD test was applied when differences were significant. In all the statistical analyses were stablished a critical level (α) of 0.05 to reject the null hypothesis.

2.3 Light microscopy

The specimens were fixed for 24 h using Davidson's fixative (ethanol absolute: seawater: formaldehyde 37 %: glycerol: glacial acetic acid in proportion 3: 3: 2: 1: 1)

and conserved in ethanol 70%. The conserved samples were processed in an automatic tissue processor (Especialidades Médicas Myr, Tarragona, Spain), then samples were embedded in paraffin using a paraffin processor (Especialidades Médicas Myr, Tarragona, Spain) to make the paraffin blocks. The paraffin blocks were sliced in 2 µm sections employing a Leica RM2155 microtome (Leica, Wetzlar, Germany). The general structure was visualized using Haematoxylin & Eosin stains; while the polysaccharides were highlighted using Periodic acid–Schiff (PAS) contrasted with Methylene Blue, and PAS combined with Alcian Blue (pH 2.5) contrasted with Hematoxylin. The protocol for the different stains was realized following Castejón (2018). The light microscopy observations were realized in a Leica LB30T 111/97 optical microscope (Leica, Wetzlar, Germany) connected to a camera (Olympus DP70 1.45 Mpx; Olympus Corporation, Germany) and image analysis software (DP Controller 2.1.1.83 and DP Manager 2.1.1.163; Olympus Corporation, Germany).

2.4 Transmission electron microscopy (TEM)

The specimens were fixed in a solution of 2% paraformaldehyde and 2.5% glutaraldehyde in cacodylate buffer (0.1 mol L^{-1} pH 7.4) during ca. 12 h at 4 °C and constant darkness. Then, the fixed specimens were washed with the same cacodylate buffer and post-fixed in 1% osmium tetroxide solution in cacodylate buffer during 90 minutes at 4 °C. The post-fixed specimens were washed again with cacodylate buffer, double-distilled water, and dehydrated in a graded series of acetone (30%, 50% and 70% realizing one time each step, followed by 90%, 95% and 100% realizing three times each step, in all cases were used 15 min step). The post-fixed and clean specimens were embedded in Spurr's resin. The semi-thin slices were obtained using a Leica UCT ultramicrotome (Leica, Wetzlar, Germany) and stained with Toluidine Blue. The ultra-thin slices were obtained using the same ultramicrotome and stained with uranyl acetate

158 and lead citrate. Observations were made with a Jeol EM-1010 transmission electron
159 microscope (tungsten filament, 80 kV). Post-fixing procedures and observations were
160 realized at Centres Científics i Tecnològics de la Universitat de Barcelona (CCiTUB;
161 Hospital Clinic, Barcelona, Spain).

3. Results

The midgut tract of of *M. brachydactyla* during the larval development is an organ positioned dorsal and anteriorly, after the stomach and before the elongated hindgut tract, below the heart. The anterior margin of the midgut tract continues dorsally with a pair of anterior caeca, medially with the stomach, and ventrally with the midgut gland (Fig. 1A–C; 2B). The posterior margin of the midgut tract continues dorsally with a single posterior caecum, and medially with the midgut-hindgut junction, which immediately continues with the hindgut tract (Figs. 1A–C; 2B-D). The midgut tract, during the entire larval development, is a short cylindrical tube from 302 ± 41 µm at hatching to 460 ± 34 µm in megalopa 11 days post-hatching (Fig. 1A–E). The midgut tract elongates significantly during the larval development following a linear model (Fig. 1D; $R^2 = 0.67$, $F_{1,71} = 144$, $p < 0.001$). The midgut tract was significantly longer during the megalopa stage than during the zoeal phases (Fig. 1E; $F_{3,17} = 21.2$, $p < 0.001$), but the maximum diameter did not vary significantly among the different stages (Fig. 1F; $F_{3,17} = 0.30$, $p = 0.83$).

Morphological organization of the midgut tract

In all the larval stages, the midgut tract of the common spider crab is lined by a simple columnar epithelium with two cell types: the digestive cells (Fig. 2), and the regenerative cells (Fig. 2A, D–E); following the nomenclature of Sonakowska et al. (2015; 2016; 2021). The digestive cells are tall columnar, dominate the epithelium, and presents microvilli in contact with the lumen (Figs. 2D–E; 3A; 4B–C; 5; 7A). Lipid droplets were observed in the cytoplasm of the main epithelial cells (Figs. 2F; 4B, D). In contrast, the regenerative cells are scarce in comparison to the digestive cells, they are small and never reach the lumen of the organ (Figs. 2D–E; 3C; 6). The epithelium is supported by a highly electron-dense and undulated basal lamina (Figs. 3C–D; 4B, E;

6A–B; 7). The basal lamina is surrounded by a thin layer formed by circular musculature which muscle fibres are visible by electron microscopy and connective tissue (Figs. 3C; 4E; 6A).

The ultrastructural study of the digestive cells do not showed clear differences when comparing between zoea I (0 days post-hatching) and megalopa (10 days post-hatching) stages. The digestive cells have a polarized organization. As mentioned before, the apical membrane forms elongated, slender and undulated microvilli that reach the lumen of the midgut tract (Figs. 2D–E; 3A; 4B–C; 5; 7A). The lateral membranes are generally straight with slight undulations (Fig. 3), showing elongated cell-to-cell junctions in the cell apex (ca. 4–5 µm; Figs. 3B–C; 4C; 5C). The basal membrane is infolded forming the basal tubular system in the basal region of the cytoplasm (Figs. 3C–D; 4B, E; 6A; 7A–B).

The apical region of the digestive cells is characterized by the presence of electron-dense vesicles which density increases towards the apical membrane (Figs. 3A–B; 4B–C; 5A–C; 7A), numerous mitochondria (Figs. 3A–B; 4B–C; 5A–B; 7A–B), and cisternae of rough endoplasmic reticulum (usually) oriented parallel to lateral cell membranes (Figs. 3B; 4B–C). The perinuclear region contains low density of organelles, consisting on sparse mitochondria and cisternae of rough endoplasmic reticulum (Figs. 3B–C; 4B, D). The basal region is dominated by the basal tubular system, a complex network of tubules formed by the basal cell membrane (Figs. 3C–D; 4B, E; 6A; 7A–B), as it is observed the fusion between the tubules and the basal cell membrane (Figs. 3D; 4E; 6A). The basal tubular system surrounds some mitochondria (Figs. 3C; 4E; 6A–B; 7B). The Golgi bodies have been observed on the apical and basal regions.

The regenerative cells are cells located near to the basis of the epithelium that never reach the midgut tract lumen due to their small size (Figs. 2D–E; 3C; 6A–B). The ultrastructure of the regenerative cells does not shown any clear polarity. Consequently, it is not possible to define any membrane or cytoplasmic region (Fig. 6A–B). The cytoplasm is lucent with ribosomes (Fig. 6). The mitochondria are small and scarce (Fig. 6A, C). The cytoplasm contains some electron-dense and lucent vesicles (Fig. 6).

Secretory activity of the midgut tract

The peritrophic membrane is present in the midgut tract already in the zoea I (ca. 12 h post-hatching), being also reported in all the posterior stages (Figs. 2C–E; 3A; 5). The peritrophic membrane is stained by Haematoxylin and PAS stains (Figs. 2C–E). The PAS combined with Alcian Blue stain revealed a remarkably stained band in the apex of the main epithelial cells, similar staining occurred in the peritrophic membrane (Fig. 2E). The position of the apical stained band observed by light microscopy (Fig. 2E) coincides with the electron-dense vesicles observed by electron microscopy (Figs. 3A–B; 4B–C; 5A–C; 7A). The content of the electron-dense vesicles is released among the microvilli following a merocrine type of secretion (Fig. 5A–C). The secretions are released through the microvilli (Figs. 3A; 5C). Near to the midgut tract lumen, a few layers composed by a highly, electron-dense, amorphous matrix are observed within the microvilli (Figs. 3A; 5D–E). The amorphous layers are sequentially wider and less electron-dense as they are released in the lumen of the midgut tract (Fig. 5D–E).

The midgut-hindgut junction

The transition between the midgut tract and the hindgut tract, the midgut-hindgut junction, is abrupt as reported by dissection (Fig. 1A–C), by light microscopy sections (Fig. 2B–D), and by transmission electron microscopy preparations (Fig. 7). Light microscopy observations reveal that the midgut-hindgut junction, in longitudinal

section, is a deep invagination created by the epithelia of both midgut and hindgut tracts (Fig. 2B–D). Each half of the invagination corresponded to the epithelia of one of the intervening organs (Fig. 2C–D). The transition itself occurs within a lapse of few cells located deeply in the invagination (Fig. 2C–D). The brush border of the midgut tract was immediately substituted by the cuticle lining of the hindgut tract (Fig. 2D).

Transmission electron microscopy confirmed the abruptness of the transition among organs in the midgut-hindgut junction (Fig. 7). Cells with mixed features of the midgut and hindgut tracts epithelia were not observed. Instead, the ultrastructure of the epithelial cells from each organ is conserved. The last digestive cell of the midgut tract reduces gradually the size of its microvilli, and the density of apical electron-dense vesicles, towards the junction (Fig. 7A–B). The basis of the last digestive cell conserves the basal tubular system and mitochondria, the folding of the basal membrane, and the electron-dense basal lamina (Fig. 7). A striking feature is the infolding of the last digestive cell basis, creating a superior cap of basal lamina that supports the first epithelial cell of the hindgut tract (Fig. 7B–C). The first epithelial cell of the hindgut tract is rounded and covered by a very thin cuticle, none other relevant feature was observed (Fig. 7B). Apparently, the cuticle is limited to the hindgut epithelial cells and does not extend towards the last digestive cell (Fig. 7B). The height of the hindgut epithelial cells and the cuticle thickness increases quickly in the next cells after the first epithelial cell of the hindgut tract (Fig. 7A).

4. Discussion

Morphology of the larval midgut tract

The midgut tract of the larval stages of the common spider crab *M. brachydactyla* is a short and simple tube positioned anteriorly, between the stomach and the hindgut tract, as observed in adults from the same species (Castejón et al., 2021). The midgut tract as

a simple tube, internally lined by a simple columnar epithelium, is shared by the larvae of several decapod taxa, including other brachyuran species (Jantrarotai and Sawanyatiputi, 2005; Spitzner et al., 2018), anomurans (Williams, 1944; Abrunhosa and Kittaka, 1997), astacideans (Factor, 1981), achelatans (Mikami et al., 1994), and carideans (Tziouveli et al., 2011; Sonakowska-Czajka et al., 2021). Major differences were found on the relative length of the midgut tract. Similarly as observed in this study, the midgut tract is a short tube in other brachyurans (Spitzner et al., 2018), and anomurans (Williams, 1944; Abrunhosa and Kittaka, 1997). On the contrary, it is a large tube reaching the sixth abdominal segment in clawed lobsters (Factor, 1981), and caridean shrimps (Tziouveli et al., 2011; Sonakowska-Czajka et al., 2021).

During the larval development of *M. brachydactyla*, the maximum length of the midgut tract increased significantly, but no differences were found on either the maximum diameter or the morphological traits of the organ. A similar developmental pattern based upon a general lengthening has been observed in the European shore crab *Carcinus maenas* (Spitzner et al., 2018), the king crab *Paralithodes camtschaticus* (Abrunhosa and Kittaka, 1997), and the shrimp *Lysmata amboinensis* (Tziouveli et al., 2011). Moreover, the gross features of the larval midgut tract of *M. brachydactyla* resembles those described in other adult decapods, including other brachyuran species (Reddy, 1937; Barker and Gibson, 1978; Erri Babu et al., 1982; Trinadha Babu et al., 1989; Kaushik and Kumar, 1998), and astacideans like crayfishes (Komuro and Yamamoto, 1968), and clawed lobsters (Yonge, 1924; Barker and Gibson, 1977). Williams (1944) reported a septum between the midgut and the hindgut junction in the pre-zoeae of the porcelain crab *Porcellana platycheles*. Such feature has not been reported by neither this nor other studies. The author postulated that the septum might disappear in the next

moult, so additional studies are required to confirm if the septum is a feature restricted to pre-hatch or embryonic stages.

Role of the larval midgut tract

The digestive cells of the midgut tract epithelium of *M. brachydactyla* showed a similar cell organization and ultrastructure in the zoea I and megalopa stages. This resemblance is interesting considering their different lifestyles: the zoeae are planktonic and free swimming stages; while the megalopae have a benthic lifestyle (Guerao et al., 2008). Moreover, the ultrastructure of the digestive cells of the midgut tract in *M. brachydactyla* larvae resembles the described in adults of different decapod species, which involves a great diversity of diets and lifestyles, e.g. true crabs (Reddy, 1937; Barker and Gibson, 1978; Erri Babu et al., 1982; Trinadha Babu et al., 1989; Kaushik and Kumar, 1998), caridean shrimps (Sonakowska et al., 2015), clawed lobsters (Barker and Gibson, 1977), and crayfishes (Komuro and Yamamoto, 1968). We propose that the conservatism of the midgut tract among life stages, taxa and diets might respond to a shared design to carry out the late phases of the digestive cycle, i.e. the biochemical processing of the food and the excretion of residuals (Icely and Nott, 1992). In comparison, the stomach is an structure with a great variation among life stages, diet and phylogeny, as it is a complex structure involved in the mechanical processing of the food (Icely and Nott, 1992; Heeren and Mitchell, 1997; Allardyce and Linton, 2010; Brösing, 2010; Brösing and Türkay, 2011; Castejón et al., 2015a; Castejón et al., 2015b; Davie et al., 2015).

The histological observations of the midgut tract of the larvae of *M. brachydactyla* revealed functionality since ca. 12 h after hatching, in which the lumen of the midgut tract is filled by the peritrophic membrane. Similar observations were realized in the larvae of clawed lobsters (Factor, 1981), and caridean shrimps (Tziouveli et al., 2011).

The peritrophic membrane is an acellular matrix present in the majority of the arthropod taxa, which separates the ingested content from the midgut and hindgut epithelia (Lehane, 1997; Boonsriwong et al., 2006). The peritrophic membrane of the decapods is composed primarily by chitin, structural proteins and several classes of enzymes (Forster, 1953; Martin et al., 2006; Wang et al., 2012). The role of the peritrophic membrane might to be a protective barrier against pathogens, abrasive particles, and toxic compounds (Barbehenn and Martin, 1992; Lehane, 1997; Terra, 2001; Martin et al., 2006; Hegedus et al., 2009; Wang et al., 2012). Wang et al. (2012) also indicated that the peritrophic membrane might assist or accelerate the digestive process, and play an important role in the gut immune system.

The midgut tract of the decapods has been traditionally considered the organ responsible of the secretion of the peritrophic membrane (Felgenhauer, 1992; Martin et al., 2006; Davie et al., 2015; Van Thuong et al., 2016). This study supports such proposal, providing evidence for secretory activity in the digestive cells of the midgut tract in larvae ca. 12 h after hatching. The secretory activity was identified as merocrine, consisting on releasing the electron-dense content of the vesicles located in the cell apex. Similarly, electron-dense vesicles sharing a similar location were also identified on the main epithelial cells of the midgut tract of adults of the dungeness crabs *Metacarcinus magister* and the clawed lobster *Homarus americanus* (Mykles, 1979), in adults of the ridgeback prawns *Sicyonia ingentis* (Martins et al., 2006); as well in the larvae of the freshwater shrimp *Neocaridina davidi* (Sonakowska-Czajka et al., 2021).

The present study showed that the content of the electron-dense vesicles apparently aggregates within the microvilli to form electron-dense layers that are sequentially released into the lumen. Following the proposal of Mykles (1979), it is tempting to suggest that the above mentioned process correspond to the formation of peritrophic

membrane layers. Georgi (1969) also reported an overlap between the weave pattern of the peritrophic membrane and the spacing of the underlying microvilli. However, Martin et al. (2006) determined that the electron-dense vesicles do not contain chitin, and were unable to identify their role. Thus, we propose that electron dense-vesicles correspond to the protein content of the peritrophic membrane, including enzymes involved in its formation and stabilization. This hypothesis is also supported by the similar staining observed between the apical band observed in the epithelial cells, and the peritrophic membrane (Fig. 2E). Consequently, the production and release of electron-dense vesicles should play an important role for the digestive physiology, specially addressing the abundance of vesicles and the ultrastructural organization of the main epithelial cells as secretory cells (Komuro and Yamamoto, 1968; Mykles, 1979).

The digestive cells of the midgut tract of *M. brachydactyla* larvae also contain lipid droplets, which were mostly observed in the megalopa stage, suggesting a role related with the absorption and storage of nutrients. The absorptive role of this organ has been suggested for species with an elongated midgut tract as shrimps (Talbot et al., 1972; Tziouveli et al., 2011), but is absent in species in which the midgut tract is vestigial as for example crayfish (Komuro and Yamamoto, 1968). The relative length of the midgut tract of *M. brachydactyla* is intermediate between the previous examples, so a complementary absorptive/storage role might be possible. The presence of a basal tubular system and mitochondria on the cell basis also suggest a potential osmoregulatory role for the midgut tract (Komuro and Yamamoto, 1968; Talbot et al., 1972).

The regenerative cells observed in the midgut tract of *M. brachydactyla* were similar to those reported in the midgut epithelium of the crayfish *Procambarus clarkii* (Komuro and Yamamoto, 1968) and the shrimp *N. heteropoda* (Sonakowska et al., 2015). The

last authors suggested these cells divide and differentiate into other cell types. Later, Sonakowska-Czajka et al. (2021) confirmed mitotic activity, supporting its role and denomination as regenerative cells.

The larval midgut-hindgut junction

The midgut-hindgut junction of the larval stages of *M. brachydactyla* is an invagination in which occurs the abrupt transition between the epithelia of the midgut tract and the hindgut tract. The transition between the midgut tract and the hindgut tract is also apparently abrupt in the larvae of *P. camtschaticus* (Abrunhosa and Kittaka, 1997) and *H. americanus* (Factor, 1981), but further detailed studies are required. Barker and Gibson (1978) mentioned that the midgut-hindgut junction contains cells with mixed features of the midgut and hindgut epithelia. The results obtained in this study cannot support such affirmation. In the larvae of *M. brachydactyla*, the epithelia of each organ maintain only contains the features of such organ, and epithelial cells with mixed features of the midgut and hindgut epithelia were not found. This observation is consistent with the fact that each organ originates from a different embryonic layer: endoderm for the midgut tract, and ectoderm for the hindgut tract (Felgenhauer, 1992; Icely and Nott, 1992; Davie et al., 2015), so the differentiation patterns of each embryonic layer might be conserved during the development. In this sense, the study of the midgut-hindgut junction of the ghost shrimp *Lepidophthalmus louisianensis* did not found cells with mixed features (Felder and Felgenhauer, 1993).

In conclusion, the midgut tract of the larvae of the common spider crab is functional since hatching. The midgut tract morphology suggests a similar role during the entire life cycle. The midgut tract is a secretory organ involved in high production of electron-dense vesicles and the peritrophic membrane. Moreover, the midgut tract is involved in the storage of nutrients as lipid droplets. Regenerative cells were reported. The midgut-

hindgut junction is an abrupt transition between both organs; the epithelia of each organ (midgut tract and hindgut tract) conserved its identity as probable consequence the different embryonic origin of each organ.

Declarations

Ethics approval and consent to participate

All applicable international, national, and/or institutional guidelines for the care and use of animals were followed. This article does not contain any studies with human participants performed by any of the authors.

Consent for publication

Not applicable.

Availability of data and materials

Data are available from the corresponding author upon reasonable request.

Competing interests

The authors declare that they have no competing interests.

Funding

G.G.: INIA Project (grant number RTA2011-00004-00-00) funded by Ministerio de Economía y Competitividad (Spanish Ministry of Economy and Competitiveness).
D.C.: FPI-INIA fellowship (INIA Project RTA2011-00004-00-00) funded by Ministerio de Economía y Competitividad (Spanish Ministry of Economy and Competitiveness).

Authors' contributions

D.C. realized the animal culture, sampling and dissections, light microscopy protocols and observations, electron microscopy observations, data analysis, figure assembling, and manuscript draft. G.R. provided support for the larval culture, manuscript revision,

and project elaboration. E.R. provided support and materials for the histology protocols, revision of the microscopy observations and interpretations, manuscript revision. M.D. provided support and materials for the histology protocols, manuscript revision. G.G. is the principal investigator, provided support for the larval culture, manuscript revision, and project elaboration. All authors reviewed the manuscript.

Acknowledgements

The authors thank the technicians at IRTA in Sant Carles de la Ràpita (David Carmona, Glòria Macià, Magda Monllaó, Francesc X. Ingla and Olga Bellot) and at CCiTUB in Hospital Clinic, Barcelona (Adriana Martínez, Almudena García, José Manuel Rebled, Rosa Rivera) for their assistance.

Bibliography

Abelló, P., García Raso, J.E., Guerao, G., Salmerón, F., 2014. *Maja brachydactyla* (Brachyura: Majidae) in the western Mediterranean. Marine Biodiversity Records 7.

Abrunhosa, F.A., Kittaka, J., 1997. Morphological changes in the midgut, midgut gland and hindgut during the larval and postlarval development of the red king crab *Paralithodes camtschaticus*. Fisheries Science 63, 746-754.

Allardyce, B.J., Linton, S.M., 2010. Functional morphology of the gastric mills of carnivorous, omnivorous, and herbivorous land crabs. Journal of Morphology 271, 61-72.

Barbehenn, R.V., Martin, M.M., 1992. The protective role of the peritrophic membrane in the tannin-tolerant larvae of *Orgyia leucostigma* (Lepidoptera). Journal of Insect Physiology 38, 973-980.

Barker, P.L., Gibson, R., 1977. Observations on the feeding mechanism, structure of the gut, and digestive physiology of the european lobster *Homarus gammarus* (L.) (Decapoda: Nephropidae). Journal of Experimental Marine Biology and Ecology 26, 297-324.

Barker, P.L., Gibson, R., 1978. Observations on the structure of the mouthparts, histology of the alimentary tract, and digestive physiology of the mud crab *Scylla serrata* (Forskål) (Decapoda: Portunidae). Journal of Experimental Marine Biology and Ecology 32, 177-196.

Bonaldo, A., Roem, A.J., Pecchini, A., Grilli, E., Gatta, P.P., 2006. Influence of dietary soybean meal levels on growth, feed utilization and gut histology of Egyptian sole (*Solea aegyptiaca*) juveniles. Aquaculture 261, 580-586.

Boonsriwong, W., Sukontason, K., Olson, J.K., Vogtsberger, R.C., Chaithong, U., Kuntalue, B., Ngern-klun, R., Upakut, S., Sukontason, K.L., 2006. Fine structure of the alimentary canal of the larval blow fly *Chrysomya megacephala* (Diptera: Calliphoridae). Parasitology Research 100, 561.

Brösing, A., 2010. Recent developments on the morphology of the brachyuran foregut ossicles and gastric teeth. Zootaxa 2510, 1-44.

Brösing, A., Türkay, M., 2011. Gastric teeth of some thoracotreme crabs and their contribution to the brachyuran phylogeny. Journal of Morphology 272, 1109-1115.

Castejón, D., 2018. Morfología del sistema digestivo y larvicultura del centollo (*Maja brachydactyla*, Balss 1922), Facultat de Biologia. Universitat de Barcelona, Barcelona, p. 798.

Castejón, D., Alba-Tercedor, J., Rotllant, G., Ribes, E., Durfort, M., Guerao, G., 2018a. Micro-computed tomography and histology to explore internal morphology in decapod larvae. Scientific Reports 8, 14399.

Castejón, D., Ribes, E., Durfort, M., Rotllant, G., Guerao, G., 2015a. Foregut morphology and ontogeny of the mud crab *Dyspanopeus sayi* (Smith, 1869) (Decapoda, Brachyura, Panopeidae). Arthropod Structure & Development 44, 33-41.

Castejón, D., Rotllant, G., Alba-Tercedor, J., Font-i-Furnols, M., Ribes, E., Durfort, M., Guerao, G., 2019a. Morphology and ultrastructure of the midgut gland ("hepatopancreas") during ontogeny in the common spider crab *Maja brachydactyla* Balss, 1922 (Brachyura, Majidae). Arthropod Structure & Development 49, 137-151.

Castejón, D., Rotllant, G., Alba-Tercedor, J., Ribes, E., Durfort, M., Guerao, G., 2022. Morphological and histological description of the midgut caeca in true crabs (Malacostraca: Decapoda: Brachyura): origin, development and potential role. BMC Zoology 7, 9.

Castejón, D., Rotllant, G., Ribes, E., Durfort, M., Guerao, G., 2015b. Foregut morphology and ontogeny of the spider crab *Maja brachydactyla* (Brachyura, Majoidea, Majidae). Journal of Morphology 276, 1109-1122.

Castejón, D., Rotllant, G., Ribes, E., Durfort, M., Guerao, G., 2018b. Morphology and ultrastructure of the esophagus during the ontogeny of the spider crab *Maja brachydactyla* (Decapoda, Brachyura, Majidae). Journal of Morphology 279, 710-723.

Castejón, D., Rotllant, G., Ribes, E., Durfort, M., Guerao, G., 2019b. Structure of the stomach cuticle in adult and larvae of the spider crab *Maja brachydactyla* (Brachyura, Decapoda). Journal of Morphology 280, 370-380.

Castejón, D., Rotllant, G., Ribes, E., Durfort, M., Guerao, G., 2021. Description of the larval and adult hindgut tract of the common spider crab *Maja brachydactyla* Balss, 1922 (Brachyura, Decapoda, Malacostraca). Cell and Tissue Research 384, 703-720.

Ceccaldi, H.J., 1989. Anatomy and physiology of digestive tract of Crustaceans Decapods reared in aquaculture, Advances in Tropical Aquaculture, Workshop at Tahiti, French Polynesia. Actes de colloques Ifremer, Tahiti, French Polynesia, pp. 243-259.

Clark, P.F., 1986. The larval stages of *Maja squinado* (Herbst, 1788) (Crustacea: Brachyura: Majidae) reared in the laboratory. Journal of Natural History 20, 825-836.

Davie, P.J.F., Guinot, D., Ng, P.K.L., 2015. Anatomy and functional morphology of Brachyura, in: Castro, P., Davie, P.J.F., Guinot, D., Schram, F., Von Vaupel Klein, C. (Eds.), Treatise on Zoology - Anatomy Taxonomy Biology. The Crustacea Volume 9 Part C. Brill, pp. 11-163.

Erri Babu, D., Shyamasundari, K., Rao, K.H., 1982. Studies on the digestive system of the crab *Menippe rumphii* (Fabricius) (Crustacea:Brachyura). Journal of Experimental Marine Biology and Ecology 58, 175-191.

Factor, J.R., 1981. Development and metamorphosis of the digestive system of larval lobsters, *Homarus americanus* (Decapoda: Nephropidae). Journal of Morphology 169, 225-242.

Factor, J.R., 1995. The Digestive System, In: Factor, J.R. (Ed.), Biology of the Lobster *Homarus americanus*. Academic Press, pp. 395-440.

Felder, D.L., Felgenhauer, B.E., 1993. Morphology of the midgut–hindgut juncture in the ghost shrimp *Lepidophthalmus louisianensis* (Schmitt) (Crustacea: Decapoda: Thalassinidea). Acta Zoologica 74, 263-276.

Felgenhauer, B.E., 1992. Chapter 3. Internal Anatomy of the Decapoda: An Overview, In: Harrison, F.W., Humes, A.G. (Eds.), Microscopic Anatomy of Invertebrates. Volume 10: Decapod Crustacea. Wiley-Liss, Inc., pp. 45-75.

Fontagné, S., Geurden, I., Escaffre, A.-M., Bergot, P., 1998. Histological changes induced by dietary phospholipids in intestine and liver of common carp (*Cyprinus carpio* L.) larvae. Aquaculture 161, 213-223.

Forster, G.R., 1953. Peritrophic membranes in the Caridea (Crustacea Decapoda). Journal of the Marine Biological Association of the United Kingdom 32, 315-318.

Fox, J., Weisberg, S., 2019. An {R} Companion to Applied Regression. Sage, Thousand Oaks {CA}.

Freire, J., Bernárdez, C., Corgos, A., Fernández, L., González-Gurriarán, E., Sampedro, M.P., Verísimo, P., 2002. Management strategies for sustainable invertebrate fisheries in coastal ecosystems of Galicia (NW Spain). Aquatic Ecology 36, 41-50.

Georgi, R., 1969. Bildung peritrophischer Membranen von Decapoda. Zeitschrift für Zellforschung und Mikroskopische Anatomie 99, 570-607.

Gibson, R., Barker, P.L., 1979. The Decapod Hepatopancreas. Oceanography and Marine Biology - An Annual Review 17, 285-346.

Guerao, G., Pastor, E., Martin, J., Andrés, M., Estévez, A., Grau, A., Duran, J., Rotllant, G., 2008. The larval development of *Maja squinado* and *M. brachydactyla* (Decapoda, Brachyura, Majidae) described from plankton collected and laboratory-reared material. Journal of Natural History 42, 2257-2276.

Guerao, G., Simeó, C.G., Anger, K., Urzúa, Á., Rotllant, G., 2012. Nutritional vulnerability of early zoea larvae of the crab *Maja brachydactyla* (Brachyura, Majidae). Aquatic Biology 16, 253-264.

Heeren, T., Mitchell, B.D., 1997. Morphology of the mouthparts, gastric mill and digestive tract of the giant crab, *Pseudocarcinus gigas* (Milne Edwards) (Decapoda: Oziidae). Marine and Freshwater Research 48, 7-18.

Hegedus, D., Erlandson, M., Gillott, C., Toprak, U., 2009. New Insights into peritrophic matrix synthesis, architecture, and function. Annual Review of Entomology 54, 285-302.

Holliday, C.W., Mykles, D.L., Terwilliger, R.C., Dangott, L.J., 1980. Fluid secretion by the midgut caeca of the crab, *Cancer magister*. Comparative Biochemistry and Physiology Part A: Physiology 67, 259-263.

Icely, J.D., Nott, J.A., 1992. Chapter 6. Digestion and Absorption: Digestive System and Associated Organs, In: Harrison, F.W., Humes, A.G. (Eds.), Microscopic Anatomy of Invertebrates. Volume 10: Decapod Crustacea. Wiley-Liss, Inc., pp. 45-75.

Jantrarotai, P.N., Sawanyatiputi, S.A., 2005. Histological study on the development of digestive system in zoeal stages of mud crab (*Scylla olivacea*). Kasetsart Journal 39, 666-671.

Kaushik, N., Kumar, S., 1998. Midgut pathology of aldrin, monocrotophos, and carbaryl in the freshwater crab, *Paratelphusa masoniana* (Henderson). Bulletin of Environmental Contamination and Toxicology 60, 480-486.

Komuro, T., Yamamoto, T., 1968. Fine structure of the epithelium of the gut in the crayfish (*Procambarus clarkii*) with special reference to the cytoplasmic microtutubles. Archivum histologicum japonicum 30, 17-32.

Lehane, M.J., 1997. Peritrophic matrix structure and function. Annual Review of Entomology 42, 525-550.

Lovett, D.L., Felder, D.L., 1989. Ontogeny of gut morphology in the white shrimp *Penaeus setiferus* (Decapoda, Penaeidae). Journal of Morphology 201, 253-272.

Martin, G.G., Rubin, N., Swanson, E., 2004. *Vibrio parahaemolyticus* and *V. harveyi* cause detachment of the epithelium from the midgut trunk of the penaeid shrimp *Sicyonia ingentis*. Diseases of Aquatic Organisms 60, 21-29.

Martin, G.G., Simcox, R., Nguyen, A., Chilingaryan, A., 2006. Peritrophic membrane of the penaeid shrimp *Sicyonia ingentis*: structure, formation, and permeability. The Biological Bulletin 211, 275-285.

Martins, G.F., Neves, C.A., Campos, L.A.O., Serrão, J.E., 2006. The regenerative cells during the metamorphosis in the midgut of bees. Micron 37, 161-168.

Mikami, S., Greenwood, J.G., Takashima, F., 1994. Functional morphology and cytology of the phyllosomal digestive system of *Ibacus ciliatus* and *Panulirus japonicus* (Decapoda, Scyllaridae and Palinuridae). Crustaceana 67, 212-225.

Milne-Edwards, H., 1834. Histoire naturelle des crustacés: atlas. Libraire Encyclopédique de Roret.

Mykles, D.L., 1979. Ultrastructure of alimentary epithelia of lobsters, *Homarus americanus* and *H. gammarus*, and crab, *Cancer magister*. Zoomorphologie 92, 201-215.

Nakamura, K., Seki, K., 1990. Organogenesis during metamorphosis in the prawn *Penaeus japonicus*. Nippon Suisan Gakkaishi 56, 1413-1417.

Øverland, M., Sørensen, M., Storebakken, T., Penn, M., Krogdahl, Å., Skrede, A., 2009. Pea protein concentrate substituting fish meal or soybean meal in diets for Atlantic salmon (*Salmo salar*)—Effect on growth performance, nutrient digestibility, carcass composition, gut health, and physical feed quality. Aquaculture 288, 305-311.

R Development Core Team, 2021. R: A language and environment for statistical computing. R Foundation for Statistical Computing, Vienna, Austria.

Reddy, A.R., 1937. The physiology of digestion and absorption in the crab *Paratelphusa* (*Oziotelphusa*) *hydrodromus* (Herbst). Proceedings of the Indian Academy of Sciences - Section B 6, 170-193.

Rotllant, G., Moyano, F.J., Andrés, M., Estévez, A., Díaz, M., Gisbert, E., 2010. Effect of delayed first feeding on larval performance of the spider crab *Maja brachydactyla* assessed by digestive enzyme activities and biometric parameters. Marine Biology 157, 2215-2227.

Schlegel, C., 1911. Anatomie sommaire de la première zoé de *Maja squinado* Latr. (Note préliminaire à des recherches sur l'Organogénese des Décapodes brachyoures). Archives de Zoologie Experimentale et Générale 5º Série T. VIII., 29-40.

Sonakowska-Czajka, L., Śróbka, J., Ostróżka, A., Rost-Roszkowska, M., 2021. Postembryonic development and differentiation of the midgut in the freshwater shrimp *Neocaridina davidi* (Crustacea, Malacostraca, Decapoda) larvae. Journal of Morphology 282, 48-65.

Sonakowska, L., Włodarczyk, A., Poprawa, I., Binkowski, M., Śróbka, J., Kamińska, K., Kszuk-Jendrysik, M., Chajec, Ł., Zajusz, B., Rost-Roszkowska, M.M., 2015. Structure and Ultrastructure of the endodermal region of the alimentary tract in the freshwater shrimp *Neocaridina heteropoda* (Crustacea, Malacostraca). PLoS ONE 10, e0126900.

Sonakowska, L., Włodarczyk, A., Wilczek, G., Wilczek, P., Student, S., Rost-Roszkowska, M.M., 2016. Cell death in the epithelia of the intestine and hepatopancreas in *Neocaridina heteropod*a (Crustacea, Malacostraca). PLoS ONE 11, e0147582.

Sotelo, G., Morán, P., Fernández, L., Posada, D., 2008a. Genetic variation of the spiny spider crab *Maja brachydactyla* in the northeastern Atlantic. Marine Ecology Progress Series 362.

Sotelo, G., Morán, P., Posada, D., 2008b. Genetic identification of the northeastern Atlantic spiny spider crab as *Maja brachydactyla* Balss, 1922. Journal of Crustacean Biology 28, 76-81.

Spitzner, F., Meth, R., Krüger, C., Nischik, E., Eiler, S., Sombke, A., Torres, G., Harzsch, S., 2018. An atlas of larval organogenesis in the European shore crab *Carcinus maenas* L. (Decapoda, Brachyura, Portunidae). Frontiers in Zoology 15, 27.

Talbot, P., Clark, W.H., Lawrence, A.L., 1972. Fine structure of the midgut epithelium in the developing brown shrimp, *Penaeus aztecus*. Journal of Morphology 138, 467-485.

Terra, W.R., 2001. The origin and functions of the insect peritrophic membrane and peritrophic gel. Archives of Insect Biochemistry and Physiology 47, 47-61.

Trinadha Babu, B., Shyamasundari, K., Hanumantha Rao, K., 1989. Observations on the morphology and histochemistry of the midgut and hindgut of *Portunus sanguinolentus* (Herbst) (Crustaceans: Brachyura). Folia Morphologica 37, 373-381.

Tziouveli, V., Bastos-Gomez, G., Bellwood, O., 2011. Functional morphology of mouthparts and digestive system during larval development of the cleaner shrimp *Lysmata amboinensis* (de Man, 1888). Journal of Morphology 272, 1080-1091.

Van Thuong, K., Van Tuan, V., Li, W., Sorgeloos, P., Bossier, P., Nauwynck, H., 2016. Per os infectivity of white spot syndrome virus (WSSV) in white-legged shrimp (*Litopenaeus vannamei*) and role of peritrophic membrane. Veterinary Research 47, 39.

Wang, L., Li, F., Wang, B., Xiang, J., 2012. Structure and partial protein profiles of the peritrophic membrane (PM) from the gut of the shrimp *Litopenaeus vannamei*. Fish & Shellfish Immunology 33, 1285-1291.

Williams, R.L., 1944. The pre-zoea stage of *Porcellana platycheles* (Pennant). Preliminary anatomical and histological notes. Journal of the Royal Microscopical Society 64, 1-15.

Yonge, C.M., 1924. Studies on the comparative physiology of digestion II. - The mechanism of feeding, digestion, and assimilation in *Nephrops norvegicus*. British Journal of Experimental Biology 1, 343-389.

600 Figure Legends

601 Figure Legends

602 Figure 1. *Maja brachydactyla*. Gross morphology and development of the midgut tract
603 during the larval development. Dissected midgut tract and associated caeca, scale bar =
604 100 µm (A–C): zoea I 0 days post-hatching, lateral view (A), zoea II 4 days post-
605 hatching, lateral view (B), and megalopa 9 days post-hatching, ventral view (C).
606 Variation of the midgut tract length during the larval development (D). Size of the
607 midgut tract in different larval stages, different letters indicate significant differences (p
608 < 0.05) (E–F): length (E) and diameter (F). Abbreviations: AC, anterior caeca; arrow,
609 midgut-hindgut junction; HGT, hindgut tract; M6d, megalopa 6 days post-hatching;
610 M11d, megalopa 11 days post-hatching; MGE, midgut tract epithelium; MGT, midgut
611 tract; PC, posterior caecum; ZI0d, zoea I 0 days post-hatching; ZII3d, zoea II 3 days
612 post-hatching.

613 Figure 2. *Maja brachydactyla*. Tissue organization of the larval midgut tract. General
614 diagram of the midgut tract (A). Midgut tract, longitudinal section (B-D): zoea I (3 days
615 post-hatching), general view, Haematoxylin-Eosin, scale bar = 50 µm (B); zoea I (0
616 days post-hatching), peritrophic membrane and midgut-hindgut junction, Haematoxylin-
617 Eosin, scale bar = 20 µm (C); zoea II (7 days post-hatching), epithelium and midgut-
618 hindgut junction, PAS contrasted with Methylene Blue, scale bar = 20 µm (D). Midgut
619 tract, transversal section, scale bar = 20 µm. (E–F): zoea I (2 days post-hatching),
620 epithelium and peritrophic membrane, PAS and Alcian Blue pH 2.5 contrasted with
621 Haematoxylin (E); megalopa (10 days post-hatching), epithelium with lipid droplets,
622 Osmium Tetroxide and Toluidine Blue (F). Abbreviations: AC, anterior midgut caecum;
623 arrow, midgut- hindgut junction; asterisk, apical stained band of the epithelial cells; BL,
624 basal lamina; C, cuticle; CT, connective tissue; DC, digestive cells (midgut tract); H,

hearth; LD, lipid droplets; MF, muscle fibres; MGE, midgut gland epithelium; MGG, midgut gland (a.k.a. hepatopancreas); MGT, midgut tract; Mv, microvilli; PC, posterior midgut caecum; PM, peritrophic membrane; RC, regenerative cells (midgut tract); SE, stomach epithelium; St, stomach.

Figure 3. *Maja brachydactyla*. Zoea I (0 days post-hatching). Midgut tract. Ultrastructure of the digestive cells. Cell apex and microvilli of the epithelial cells, scale bar = 500 nm (A). Apical and perinuclear region of the digestive cells, scale bar = 2 µm (B). Perinuclear and basal region of the digestive cells and regenerative cell, scale bar = 4 µm (C). Basal tubular system of the digestive cells and basal lamina, scale bar = 500 nm (D). Abbreviations: arrowheads, secretions located through the microvilli; BL, basal lamina; BTS, basal tubular system; EV, electron-dense vesicles (cytoplasm); LV, lucent vesicles (cytoplasm); Mt, mitochondria; Mv, microvilli; My, myofibrils; N, nucleus; numbers (1–2), layers of secretion of peritrophic membrane; RC, regenerative cell; RER, rough endoplasmic reticulum.

Figure 4. *Maja brachydactyla*. Megalopa (10 days post-hatching). Midgut tract. Ultrastructure of the digestive cells. General diagram (A). General view of the digestive cells, scale bar = 5 µm (B). Apical region of the digestive cells, scale bar = 1 µm (C). Perinuclear region of the digestive cells, scale bar = 1 µm (D). Basal tubular system and basal region of the digestive cells, detail of the basal lamina, scale bar = 1 µm (E). Abbreviations: asterisk, cell-to-cell junction; BL, basal lamina; BTS, basal tubular system; EV, electron-dense vesicles (cytoplasm); LD, lipid droplets; Mt, mitochondria; Mv, microvilli; My, myofibrils; N, nucleus; RER, rough endoplasmic reticulum.

Figure 5. *Maja brachydactyla*. Larval midgut tract. Secretory activity of the digestive cells. Megalopa (10 days post-hatching), mecrocrine secretion (A–B): scale bar = 1 µm (A), scale bar = 500 nm (B). Zoea I (0 days post-hatching), scale bar = 500 nm (C–E):

mecrocrine secretion (C); layers of secretion of peritrophic membrane through the microvilli (numbers 1 to 2) (D); layers of secretion of peritrophic membrane (numbers 1 to 5) (E). Abbreviations: arrowheads, fusion between the apical membrane and the electron-dense vesicles; arrows, secretions located through the microvilli; asterisk, cell-to-cell junction; EV, electron-dense vesicles (cytoplasm); Mt, mitochondria; Mv, microvilli; numbers (1-5), layers of secretion of peritrophic membrane.

Figure 6. *Maja brachydactyla*. Zoea I (0 days post-hatching). Ultrastructure of the regenerative cells. General view, scale bar = 2 µm (A–B). Detailed view of the lucent vesicles and mitochondria, scale bar = 500 nm (C). Abbreviations: BL, basal lamina; BTS, basal tubular system; EV, electron-dense vesicles (cytoplasm); LV, lucent vesicles (cytoplasm); Mt, mitochondria; My, myofibrils; N, nucleus.

Figure 7. *Maja brachydactyla*. Megalopa (10 days post-hatching). Midgut-hindgut junction. General view, scale bar = 5 µm (A). Detailed view of the last digestive cell of the midgut tract and the first hindgut tract epithelial cell, scale bar = 1 µm (B). Transition of the basal lamina, scale bar = 2 µm (C). Abbreviations: BL, basal lamina; BTS, basal tubular system; C, cuticle; CE, potential end of the cuticle; DC, digestive cells of the midgut tract; FHE, first hindgut tract epithelial cell; HE, hindgut tract epithelial cells; LDC, last digestive cell of the midgut tract; Mt, mitochondria; Mv, microvilli.

Figure 1

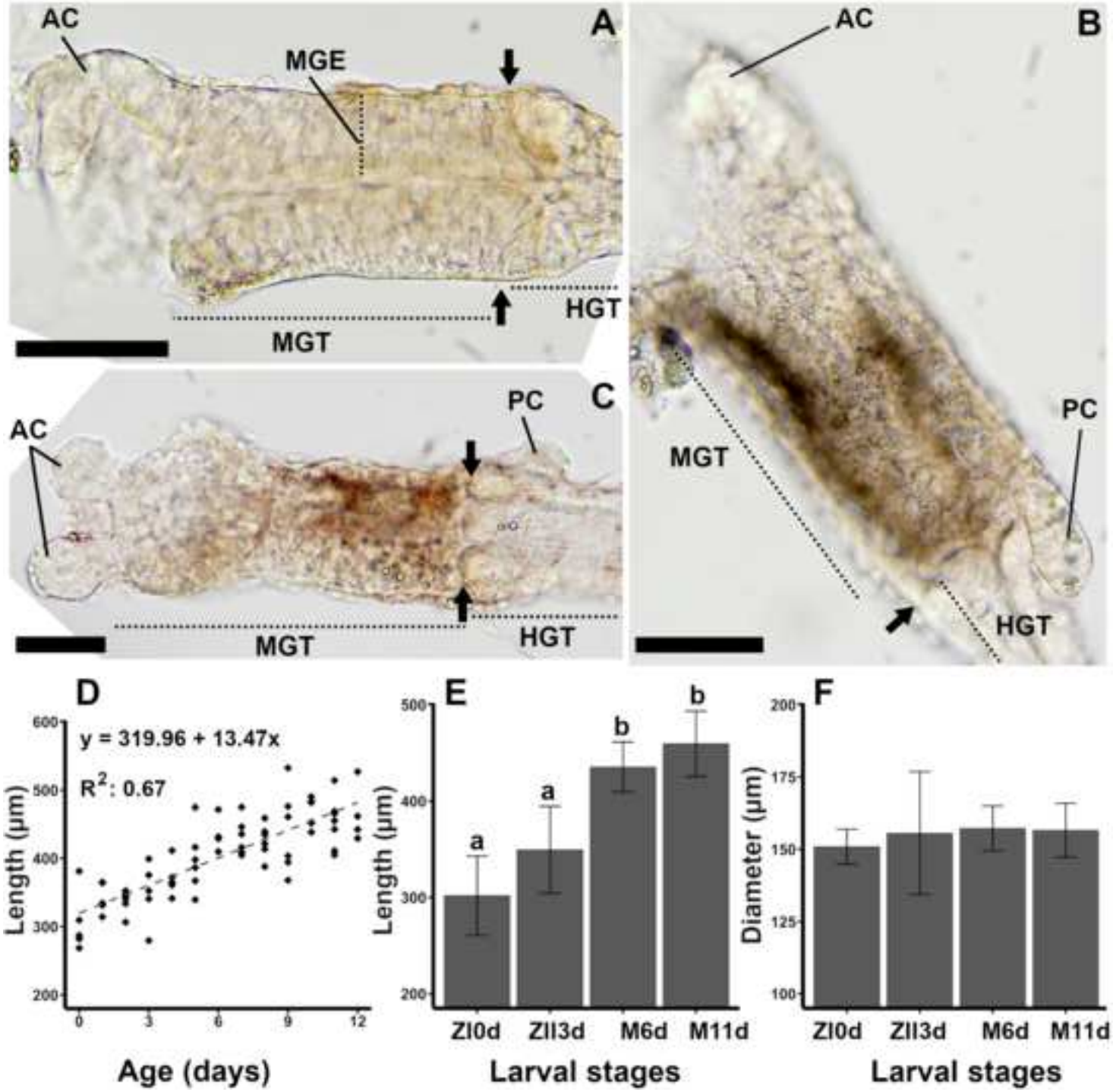
A
AC
MGE
HGT
MGT
B
AC
PC
MGT
HGT
C
AC
PC
MGT
HGT
D
y = 319.96 + 13.47x
R2: 0.67
Length (µm)
Age (days)
E
Length (µm)
a
a
b
b
ZI0d
ZII3d
M6d
M11d
Larval stages
F
Diameter (µm)
ZI0d
ZII3d
M6d
M11d
Larval stages

Figure 2

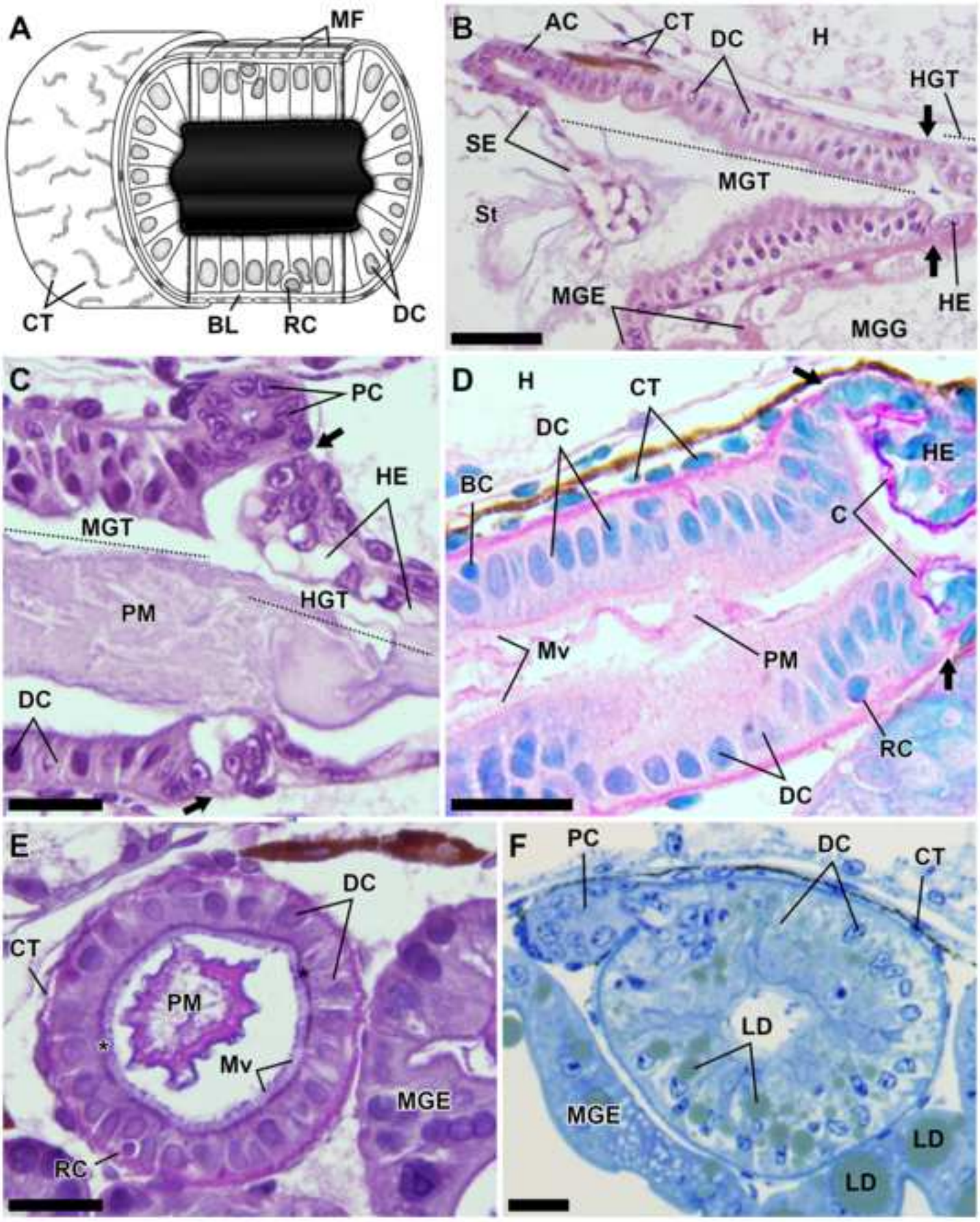
A
MF
CT
BL
RC
DC
B
AC
CT
DC
H
HGT
SE
MGT
St
MGE
HE
MGG
C
PC
HE
MGT
HGT
PM
DC
D
H
CT
DC
HE
BC
C
Mv
PM
RC
DC
E
DC
CT
PM
Mv
MGE
RC
F
PC
DC
CT
LD
MGE
LD
LD

Figure 3

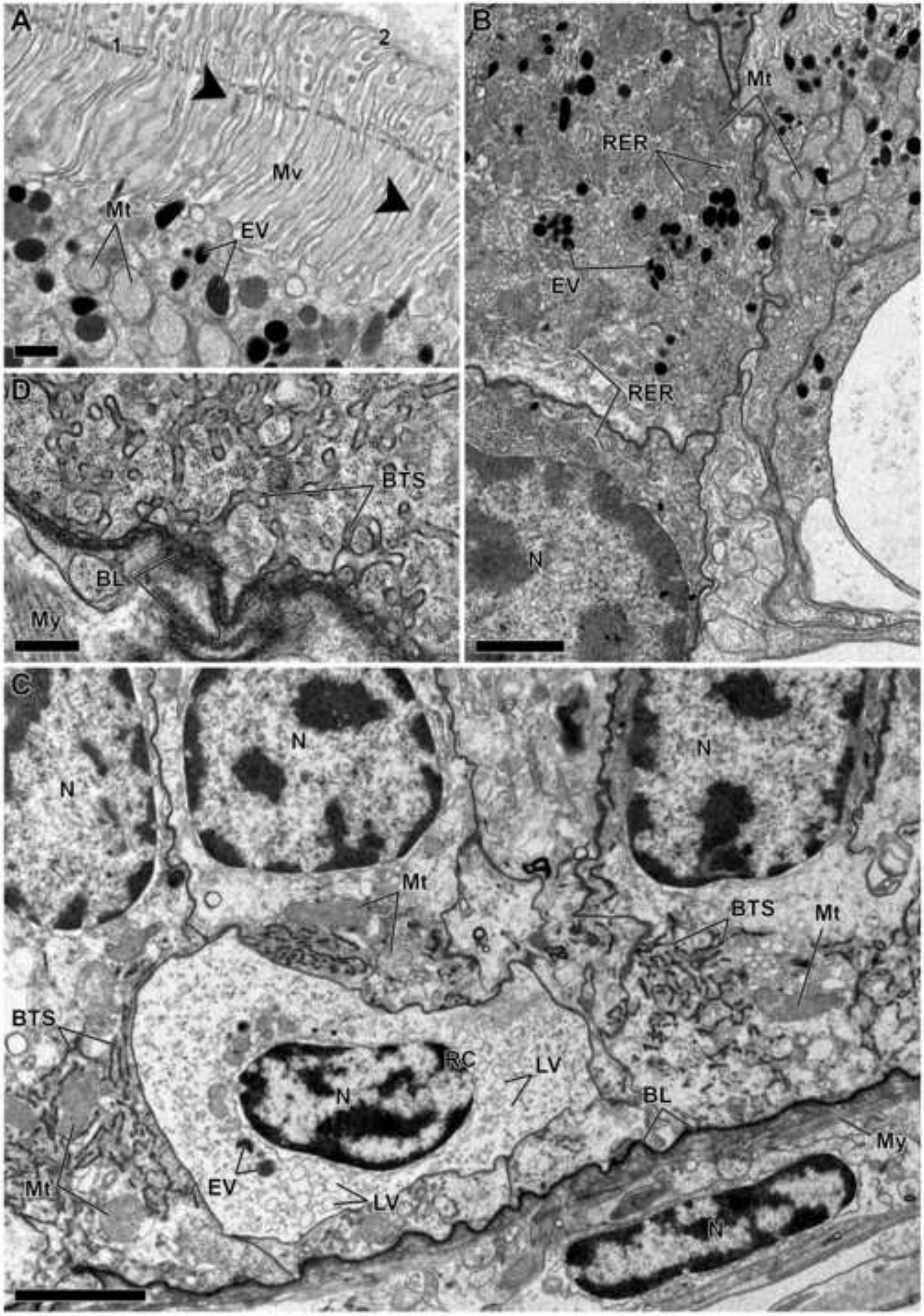
A
1
2
Mv
Mt
EV
B
Mt
RER
EV
RER
N
D
BTS
BL
My
C
N
N
N
Mt
BTS
Mt
BTS
RC
LV
N
BL
My
Mt
EV
LV
N

Figure 4

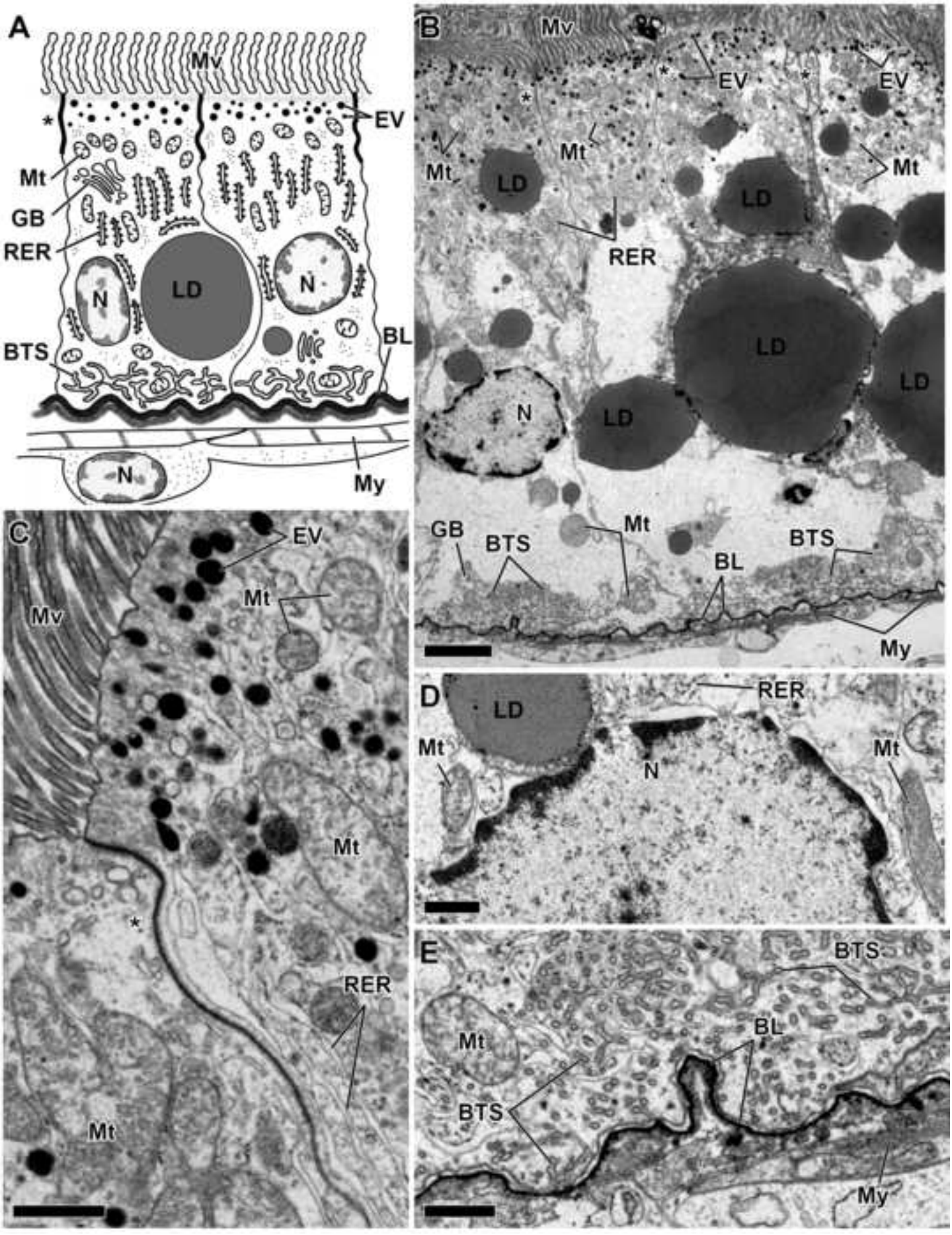
A
Mv
EV
Mt
GB
RER
N
LD
N
BTS
BL
N
My
B
Mv
EV
EV
Mt
Mt
Mt
LD
LD
RER
LD
LD
N
LD
GB
BTS
Mt
BTS
BL
My
C
EV
Mv
Mt
Mt
RER
Mt
D
RER
LD
Mt
N
Mt
E
BTS
Mt
BL
BTS
My

Figure 5

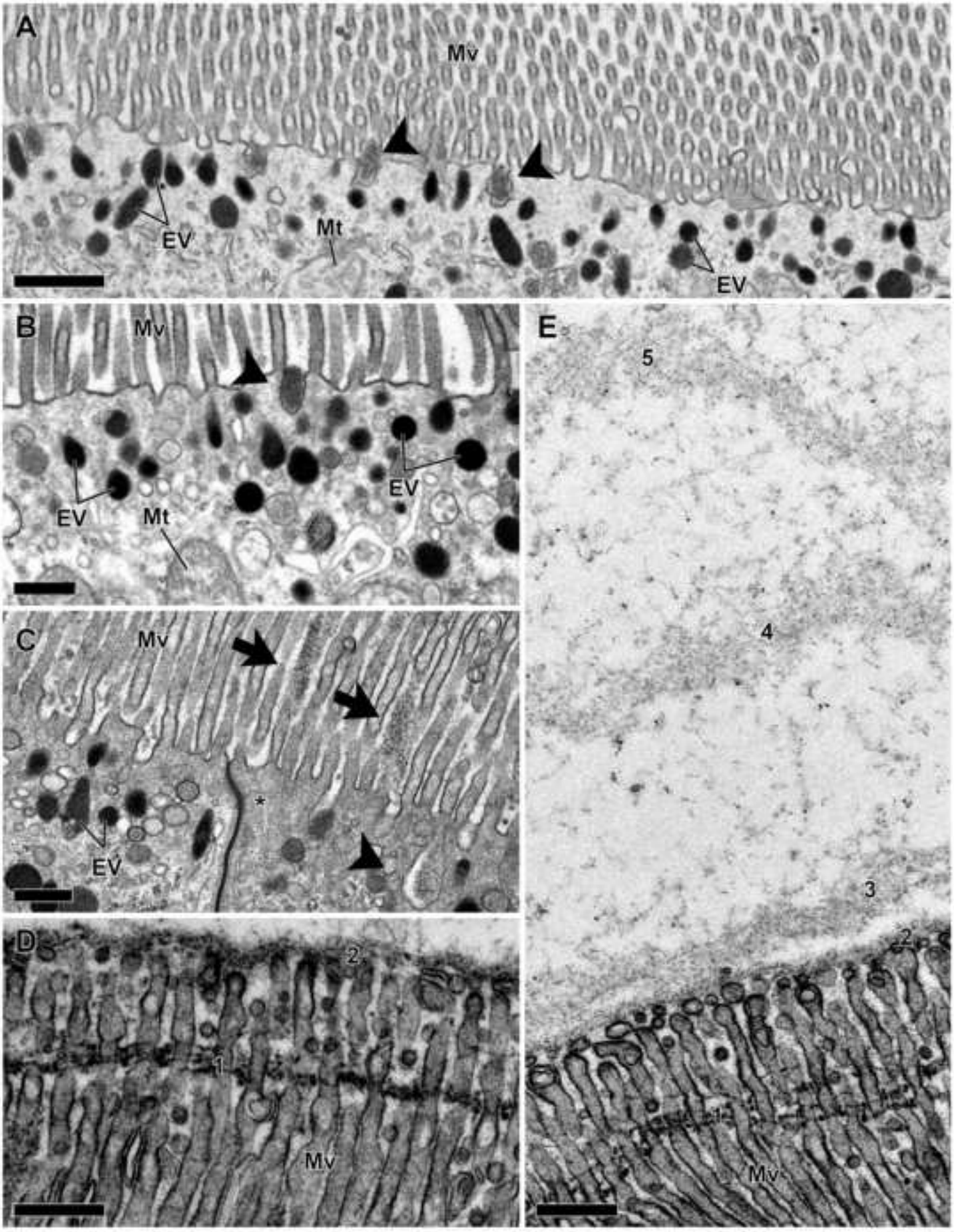

Figure 6

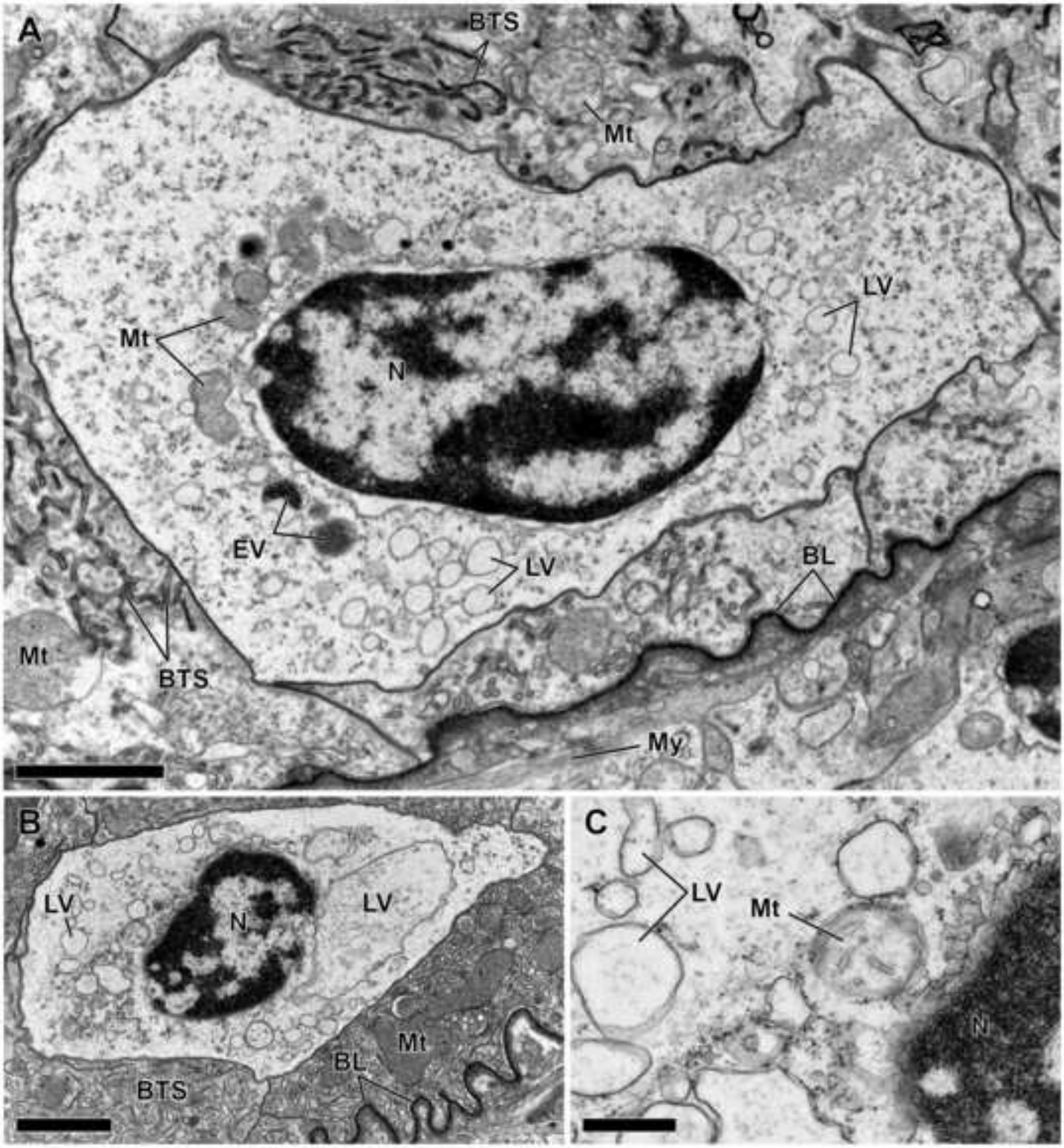

Figure 7

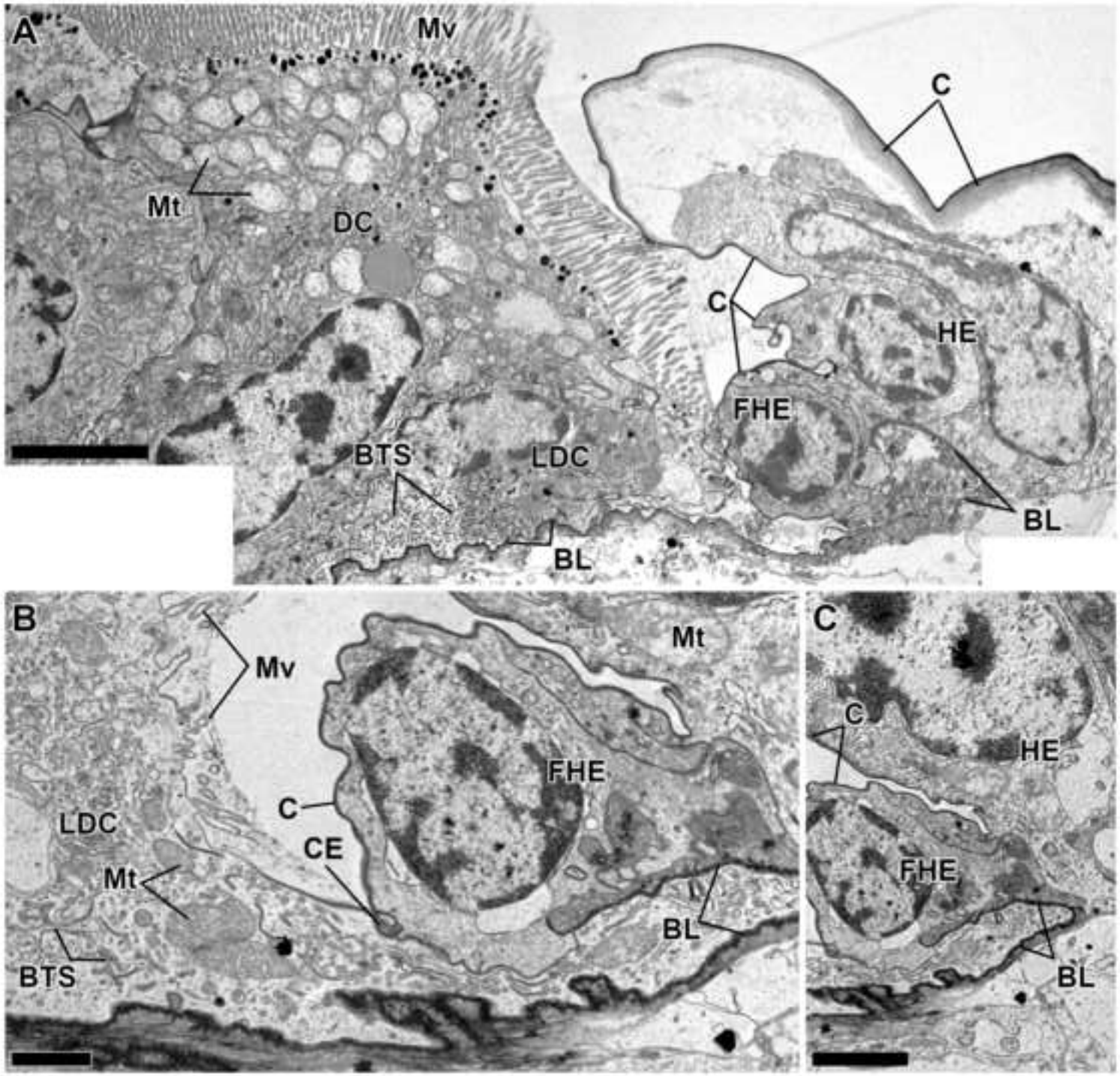
A
Mv
C
Mt
DC
C
HE
FHE
BTS
LDC
BL
BL
B
Mv
Mt
FHE
C
LDC
CE
Mt
BL
BTS
C
C
HE
FHE
BL